Published in final edited form as:
Mol Cancer Res. 2012 March ; 10(3): 469–482. doi:10.1158/1541-7786.MCR-11-0177.

WNT7A regulates tumor growth and progression in ovarian cancer through the WNT/β-catenin pathway

Shin Yoshioka[1], **Mandy L. King**[1], **Sophia Ran**[2], **Hiroshi Okuda**[2], **James A. MacLean II**[1], **Mary E. McAsey**[3], **Norihiro Sugino**[4], **Laurent Brard**[3], **Kounosuke Watabe**[2], and **Kanako Hayashi**[1]

[1]Department of Physiology, Southern Illinois University School of Medicine, Carbondale, IL 62901

[2]Department of Medical Microbiology, Immunology and Cell Biology, Southern Illinois University School of Medicine, Carbondale, IL 62901

[3]Department of Obstetrics and Gynecology, Southern Illinois University School of Medicine, Carbondale, IL 62901

[4]Department of Obstetrics and Gynecology, Yamaguchi University Graduate School of Medicine, Ube, Japan 755-8505

Abstract

Abnormal activation the WNT/β-catenin signaling pathway has been associated with ovarian carcinomas, but a specific WNT ligand and pertinent downstream mechanisms are not fully understood. In this study, we found abundant *WNT7A* in the epithelium of serous ovarian carcinomas, but not detected in borderline and benign tumors, normal ovary or endometrioid carcinomas. To characterize the role of WNT7A in ovarian tumor growth and progression, nude mice were injected either intraperitoneally (i.p.) or subcutaneously (s.c.) with WNT7A knocked down SKOV3.ip1 and overexpressed SKOV3 cells. In the i.p. group, mice receiving SKOV3.ip1 cells with reduced WNT7A expression developed significantly fewer tumor lesions. Gross and histological examination revealed greatly reduced invasion of WNT7A knockdown cells into intestinal mesentery and serosa compared to the control cells. Tumor growth was regulated by loss or overexpression of WNT7A in mice receiving s.c. injection as well. *In vitro* analysis of cell function revealed that cell proliferation, adhesion, and invasion were regulated by WNT7A. The activity of the TCF/LEF reporter was stimulated by overexpression of WNT7A in ovarian cancer cells. Co-transfection with WNT7A and FZD5 receptor further increased activity, and this effect was inhibited by co-transfection with SFRP2, or dominant-negative TCF4. Overexpression of WNT7A stimulated MMP7 promoter, and mutation of TCF binding sites in MMP7 promoter confirmed that activation of MMP7 promoter by WNT7A was mediated by β-catenin/TCF signaling. Collectively, these results suggest that re-expression of WNT7A during malignant transformation of ovarian epithelial cells plays a critical role in ovarian cancer progression mediated by WNT/β-catenin signaling pathway.

Keywords

WNT7A; epithelial ovarian cancer; WNT/β-catenin pathway; cyclin D1; MMP7

Correspondence: Kanako Hayashi, Department of Physiology, Southern Illinois University, School of Medicine, 1135 Lincoln Drive, Carbondale, Illinois 62901. Tel: 618-453-1562, Fax: 618-453-1517, khayashi@siumed.edu.
SY and MLK contributed equally to this work.

No potential conflicts of interest were declared.

Introduction

Ovarian cancer remains the most common cause of death from a gynecological malignancy and is the fifth leading overall cause of death from cancer in women(1). Epithelial ovarian cancer (EOC) constitutes more than 90% of ovarian malignancies (2). The high mortality related to EOC is thought to be due to the advanced stage of the disease at presentation. Unlike most carcinomas that dedifferentiate during neoplastic progression, ovarian carcinomas undergo transition to a more epithelial phenotype early in tumor progression. Thus, identification of novel diagnostic and prognostic factors in EOC can aid in predicting clinical outcome.

WNT genes encode secreted glycoproteins acting through frizzled receptor (FZD) that control cell fate, mortality, proliferation, differentiation (3, 4) and tissue growth (5). WNT was initially discovered as a proto-oncogene in mammary tumors activated by integration of the mouse mammary tumor virus (6). The WNT pathway promotes ovarian cancer progression via diverse mechanisms including gene mutations and changes in expression of extracellular inhibitors and intranuclear transcription cofactors. The canonical pathway of WNT signaling results in β-catenin nuclear accumulation and transcriptional activation of target genes. In the presence of WNTs, cytoplasmic β-catenin is stabilized by inhibition of GSK3β, translocated to the nucleus where it associates with LEF/TCF transcription factors, and induces *c-myc*, *cyclinD* and *MMP7* (7–9). It has been established that the WNT pathway is often constitutively activated, usually via missense mutation of *CTNNB1* (β-catenin), in the endometrioid histopathologic type of ovarian carcinomas. These mutations typically alter residues phosphorylated by GSK3β, and hence, β-catenin protein cannot be targeted for degradation, leading to deregulation of the pathway and transcription of target genes, which are likely important for neoplastic transformation and tumor progression (10). Endometrioid adenocarcinomas with deregulated WNT signaling show nuclear accumulation of β-catenin whereas tumors with intact WNT signaling show only stromal and membrane-bound β-catenin (10, 11). However, nuclear localization of β-catenin was also observed in high percentage of both low- and high-grade serous carcinomas (12), suggesting that the WNT/β-catenin pathway can be activated in other categories of EOC without mutation of β-catenin. However, the identity and the clinical significance of the ligand partners associated with WNT signaling in ovarian cancer are currently unknown.

We focused on one of Wnt ligands, WNT7A, for several reasons. In the female reproductive tract, *WNT7A* is exclusively expressed in epithelial cells (13–17) and acts via FZD in the mesenchyme and epithelium. In rodents, *Wnt7a* regulates a variety of cellular and developmental pathways that direct prenatal growth of the female reproductive tract and maintain proper uterine function (14). Further, WNT7A increases cell proliferation via activation of the canonical WNT/β-catenin pathway (18, 19). In endometrial carcinomas, WNT7A acting via β-catenin signaling induces cell proliferation (20), where SFRP4 (a WNT receptor antagonist) suppresses the activity of WNT7A leading to inhibition of cell division (21). While WNT7A dependent regulation of cell proliferation and adhesion in other tissues and tumors has been reported, the role of WNT7A in ovarian cancer has not been examined due to the absence of WNT7A in normal ovary.

In the present study, we found that *WNT7A* is not expressed in normal adult ovarian tissues, but is highly and frequently expressed in a large panel of human malignant ovarian tumors. We also determined in an orthotopic xenograft model that suppression of WNT7A in an ovarian carcinoma line SKOV3.ip1 severely restricts establishment of tumor lesions as well as their spread throughout the peritoneal cavity. This result was supported by overexpression of WNT7A in SKOV3 cells. *In vitro* analyses showed that WNT7A controls proliferation, adhesion, invasion, and cell cycle of ovarian cancer cells. These effects were accompanied

by up-regulation of MMP7 and cyclin D1, two known transcriptional targets of the canonical β-catenin/TCF pathway. Collectively, these data demonstrate overexpression of WNT7A in human ovarian cancer, and suggest an important role for this ligand in progression of ovarian malignancies.

Materials and Methods

Tissue samples and cell lines

A total of 300 paraffin-embedded and 18 fresh-frozen tumor, benign/borderline and normal ovarian specimens were obtained from the tissue bank at Southern Illinois University School of Medicine Simmons Cancer Institute and US Biomax (Rockville, MD). Histopathological typing was verified for each section by a gynecological oncology pathologist. Human ovarian cancer cell lines: OVCAR3, SKOV3, TOV-112D, TOV-21G. OV-90, MDAH 2774 and ES2 were purchased from ATCC. A2780 was purchased from Sigma. HEY, HEYA8, OVCAR8, OVCA420, OVCA429, OVCA432 and OVCA433 were purchased from the cell bank of The University of Texas MD Anderson cancer center. All experiments using these cell lines were done within 4 months after receipt. SKOV3.ip.1 and IGROV-1 cells were kindly provided by Dr. Judith Wolf of The University of Texas MD Anderson cancer center and Dr. Laurent Brard Southern Illinois University School of Medicine, respectively. SKOV3.ip1 and IGROV-1 cell lines were initially characterized and described in *Cancer Research* (22) and (23), respectively. The cells used were from passage 14 and 21 of the original clone. The cells were characterized by measuring the expression of genes (all 19 *WNT* genes, MMP7, MMP9) and active β-catenin in nuclear extracts. The expression was consistent with the data from the original clone. All cells were tested routinely for cell proliferation and BrdU incorporation as well as mycoplasma contamination, and they showed similar growth rate and negative mycoplasma during the experiment. TOV-112D, TOV-21G, and OV-90 cells were grown in 1:1 MCDB 105:M199 with 15% FBS and penicillin/streptomycin, other cells were cultured in DMEM with 10% FBS, 200mM glutamine and penicillin/streptomycin. All cell lines were grown at 37 °C in a humidified 5% CO_2 incubator.

RNA expression analyses

Total RNA was isolated from human tissues and cells, and cDNA was synthesized from total RNA. Relative gene expression was determined by SYBR green incorporation in a Bio-Rad myCycler as described previously (16). A table of oligonucleotides used for each gene is present in Supplementary Table S1. *In situ* hybridization analysis of human ovarian tissues was conducted using methods described previously (24).

Western blot analysis

Thirty micrograms of total protein from whole cell lysates, or ten micrograms nuclear or cytoplasmic protein extract were separated on SDS-PAGE gels and transferred to nitrocellulose membranes (Millipore). Membranes were blocked and incubated overnight at 4°C with primary antibodies: anti-WNT7A (#HPA015719) from Sigma-Aldrich, anti-MMP7 (#05-665) and anti-active β-catenin (#MAB3315) from Millipore, anti-β-catenin (#610153) from BD Biosciences, anti-cyclin D1 (#RM-9104-S1) from Thermo Fisher, and anti-GAPDH (#3073) and anti-actin (#5401) from IMGENEX. Bound antibody was visualized with IRDye 700 or 800 conjugated affinity-purified secondary antibodies (Rockland Immunochemicals) using the Odyssey infrared imaging system (LI-COR).

Cell proliferation assay

To assess cell proliferation, cells (2×10^4/well) were seeded in 24-well plates and cultured in DMEM without serum for 20 h. During this incubation, cells attached to the substratum but did not proliferate. After serum-starvation for 20 h, 3 wells were harvested, stained with trypan blue to assess viability, and counted using an automated cell counter TC10 (BioRad) to serve as 0 h control. Cells in parallel wells were cultured with normal growth medium at 37 °C for 24, 48 or 72 h, and then stained with trypan blue and counted as above. In addition to counting total cell numbers, BrdU incorporation during DNA synthesis was measured after 48 h culture with growth medium following manufacturer's recommendations (Roche applied Science). Doubling time of cells was calculated from the growth rate during the exponential growth phase (0–72 h) using the formula, $Td = 0.693t/\ln(N_t/N_0)$, where t is time in days, N_t is cell number at time t, and N_0 is cell number at initial time (25, 26).

Cell cycle assay

Cells (1×10^5/well) were seeded in 6 well plates in DMEM without serum for 20 h. Synchronized cells were then cultured in growth medium for 24 h or 48 h for SKOV3.ip.1 and SKOV3 cells, respectively, before collection by trypsinization and centrifugation. Cell pellets washed with ice cold PBS were suspended in 0.5% Triton X-100 in PBS containing RNase A and propidium iodide, and incubated for 15 min on ice. Fluorescent emission was quantified by FACScan cytometry (Beckman Coulter CellQuanta).

Cell adhesion assay

Cells (4×10^4/well) were seeded in 96-well plates. After 1 h incubation for SKOV3.ip.1 cells or 2 h incubation for SKOV3 cells at 37 °C, cells were washed with PBS and fixed with 10% formaldehyde for 5 min. Fixed cells were stained with Amido Black in PBS (0.1% w/v) for 20 min at room temperature as described previously (27). The plate was immersed in water and destained by gentle shaking. Stained cells were immediately lysed in 100 μl of 2N NaOH followed by reading absorbance at 595 nm using a microplate reader (BioTek Synergy HT).

Cell invasion assay

Cell invasion assays were performed using a modified Boyden Chamber method with 8-μm pore size polycarbonate membrane 24-well transwells coated with matrigel (Corning), as previously described (18, 28, 29). Cells were serum-starved in DMEM for 20 h, dislodged, and re-plated in the upper well at a density of 75×10^3 cells per well in 100 μl of serum-free medium. After 24 h, cells remaining on the upper surface of the membrane were wiped off with a cotton swab. For evaluation of invading cells on the lower surface, inserts were fixed in 4% paraformaldehyde for 3 min. Transwell membranes were then removed and stained with DAPI. Invading cells were counted in five non-overlapping fields, which covered approximately 70% of the insert membrane area, using a Leica DM5000B photomicroscope. The results are presented as the mean number of invading cells per field ± SEM.

Orthotopic models of ovarian tumor growth and peritoneal dissemination in nude mice

To examine WNT7A loss-of-function, SKOV3.ip1 cells were infected with lentivirus containing WNT7A shRNA or control virus followed by selection of clones with stable incorporation of shRNA. Five different WNT7A shRNAs, Sigma Mission clone numbers TRCN00000621- #8, -#9, -#10, -#11 and -#12, were examined for knockdown of WNT7A in SKOV3.ip1 cells. Two individual stable WNT7A shRNA clones, for each shRNA #11 and #12, were selected based on their highest suppression of WNT7A. To examine WNT7A gain-of-function, SKOV3 cells were transfected using Turbofect, with either empty pcDNA3.1 control vector or WNT7A cloned into pcDNA3.1 vector. Stably transfected

clones were selected with G418 (600 μg/ml), expanded individually, and analyzed for WNT7A expression (clones B2 and E1 exhibited highest expression). These derivatives of the SKOV3.ip1 and SKOV3 lines were injected either i.p. (3×10^6 cells, n=5–6), or s.c. (1×10^6 cells, n=5–6) into7–8 week-old female nude mice (*nu/nu* BALB/*c*, Harlan). Body weight of mice was determined every 7 days after i.p. injection. To determine tumor dissemination in the peritoneal cavity, mice were euthanized and necropsied 5–10 weeks after the i.p. injection. Tumor lesions having 2 mm or larger diameter grown on the mesentery, omentum and abdominopelvic region were enumerated, excised and weighed. Harvested tumors were either frozen or fixed with 4% paraformaldehyde in PBS for further analysis. Subcutaneous tumor growth was monitored by volume calculated according to the formula $L\ X\ W^2/2$, where L is length and W is width (30). Tumors were measured every 2 days starting at day 10th after s.c. injection. Six-nine weeks after s.c. injection, mice were euthanized and necropsied. Harvested tumors were weighed and either frozen or fixed with 4% paraformaldehyde in PBS for further analysis.

CTNNB1 mutation analysis

DNA from fixed tissues was isolated using QIAamp DNA FFPE Tissue Kit (56404). Exon 3 has previously been shown to harbor mutations at codons 33, 34 and 37 in endometrioid ovarian cancer. To assess for these mutations in our samples, we amplified this region using primers: Forward, 5′-CGTGGACAATGGCTACTCAA -3′ and Reverse5′-TGCATACTGTCCATCAATA -3′ (31). Each PCR fragment was purified and sequenced using a Beckman CEQ 8000 DNA sequencer with GenomeLab™ DTCS Quick Start Kit and the following primer 5′-GGAGTTGGACATGGCCATGGAA -3′. Sequencing reactions were repeated for all samples.

Statistical analyses

Chi-square tests were used to compare the intensity of *WNT7A* expression in ovarian tumor specimens according to grade. Fisher's exact tests were used to determine up-regulation of *WNT7A* in each tumor subtype. Quantitative data were subjected to least-squares ANOVA and differences between individual means were tested by a Tukey multiple-range test using Prism 4.0 (Graphpad). Real-time PCR data were corrected for differences in sample loading using the *RPL19* data as a covariate. Tests of significance were performed using the appropriate error terms according to the expectation of the mean squares for error. A p-value of 0.05 or less was considered significant. Data are presented as least-square means (LSM) with standard error of the means (SEM).

Results

WNT7A is highly expressed in EOC

We used quantitative real-time PCR with primers specific for 19 human *WNT* genes to determine relative *WNT* gene expression in human ovary. Transcripts for all *WNT* genes, except *WNT1*, *WNT8B*, *WNT9B*, *WNT10A*, and *WNT16*, were detected in the ovarian tissues (n=8–10). The expression of *WNT2*, *WNT2B*, *WNT3A*, *WNT5A*, *WNT5B*, *WNT6*, *WNT8A*, *WNT9A*, *WNT10B* and *WNT11* did not exhibit significant differences in expression between biopsies taken from normal and malignant ovarian tissues (Supplementary Table S2). The levels of *WNT3* and *WNT4* were reduced by 82% and 85%, respectively ($P<0.05$), in malignant tissues. In contrast, *WNT7A* and *WNT7B* were overexpressed 398-fold and 34-fold, respectively ($P<0.05$), in malignant compared with normal ovarian tissues. *WNT7A* was selected for further analysis because it was the highest upregulated WNT ligand in malignant ovarian tissues.

To determine the potential role of WNT7A in EOC, we first examined its spatial expression by radioactive *in situ* hybridization (Fig. 1a). A total of 300 specimens including 189 serous adenocarcinomas, 52 endometrioid adenocarcinomas, 19 mucinous adenocarcinomas and 21 clear cell adenocarcinomas, as well as 12 normal ovary and 7 benign/borderlines were hybridized with human *WNT7A* cRNA probe to determine *WNT7A* localization. These results are summarized in Fig. 1b.

Weak to strong expression of *WNT7A* was observed in approximately 65% of serous adenocarcinomas. Fisher's exact test confirmed that *WNT7A* expression was up-regulated in serous carcinomas (P=0.0001). With the exception of a few specimens, *WNT7A* was not detected in endometrioid adenocarcinomas as confirmed by Fisher's exact test (P=0.58). Most mucinous and clear cell adenocarcinomas did not express *WNT7A*. The expression of *WNT7A* in these type of tumors was not statistically significant (Fisher's exact test P=0.47). Importantly, examination by a gynecological oncologist in this study revealed that *WNT7A* was detected only in the ovarian epithelium, not other cell types (Fig. 1a).

WNT7A expression in ovarian cancer cell lines

Next, we determined relative *WNT7A* expression in a panel of ovarian carcinoma cell lines with variable tumorigenic potential (Supplemental Fig. 1a). In agreement with data presented in Fig. 1, *WNT7A* was not detected in non-tumorigenic ovarian cell lines ISOE1386 and HOSE642E. Near background levels of *WNT7A* were detected in most tumorigenic cell lines. However, *WNT7A* was moderately expressed in IGROV-1 (52-fold, P<0.05). *WNT7A* was abundantly expressed (390-fold, P<0.001) in one line, SKOV3.ip1, an SKOV3 line derivative established from ascites developed in nude mice after i.p. injection (22). IGROV-1 cells expressed WNT7A above background levels, but did not possess potent activation of β-catenin signaling (1.35-fold, P<0.2, Top-Flash reporter activity) observed in SKOV3.ip1 (6.2-fold, P<0.05, data not shown). Therefore, we chose to focus on SKOV3.ip1 and their parental SKOV3 cells for further experiments. Consistent with a previous report, high *WNT7A* expression was also detected in the endometrial carcinoma cell line, HEC-1A (32).

Because SKOV3.ip1 and SKOV3 are isogenic lines, we could examine the effects of naturally occurring WNT7A overexpression on transcriptional activation of genes known to be regulated by the WNT pathway. In particular, the expression of *WNT7A*, *MMP7*, and *MMP9* was low in SKOV3 cells, but presented at high levels in SKOV3.ip1 cells. When mRNA levels in SKOV3 cells were set to a background level of 1, *WNT7A*, *MMP7*, and *MMP9* were 390-, 3200-, and 5-fold, respectively, higher in SKOV3.ip1 cells (P<0.05, Supplemental Fig. 1b). In contrast, *WNT5A* was expressed at equivalent levels in both SKOV3 and SKOV3.ip1 lines. This suggests that increased gene transcription of pro-metastatic *MMP7*, and *MMP9* metalloproteinase genes might not be a general phenomenon, but rather a result of activation of a metastasis related transcriptional program in SKOV3.ip1 cells.

WNT7A regulates cell proliferation, adhesion and invasion of ovarian cancer cells

To understand the functional significance of WNT7A in ovarian cancer cells, we generated stable human ovarian cancer cell lines, in which WNT7A was either knocked down or overexpressed. To knockdown WNT7A and examine loss-of-function, SKOV3.ip1 cells, which have high endogenous WNT7A, were used *in vitro* following shRNA gene knockdown methods. Two stable clones from #11 or #12 shRNA were selected based on puromycin resistance and western blot analysis of effective WNT7A knockdown. WNT7A was substantially depleted in clones #11 and #12 stably expressing WNT7A shRNAs compared with those infected with control shRNA (Fig. 2a). Tumor cells with reduced

expression of WNT7A also had lower expression of MMP7 and cyclin D1, suggesting that expression of both of these proteins is regulated by WNT7A signaling. To determine the effect of WNT7A overexpression, SKOV3 cells that lack endogenous WNT7A were transfected with empty vector or plasmids encoding WNT7A. Two G418-selected stable clones (B2 and E1) were used for further analysis based on WNT7A expression detected by western blot (Fig. 2a). Once again, the expression of MMP7 and cyclin D1 mirrored upregulation of WNT7A in a genetically manipulated SKOV3 line.

Using these stable cell lines, we examined the *in vitro* effects of WNT7A on cell proliferation, adhesion and invasion, using these assays as indicators of WNT7A's role in tumor growth *in vivo* (Fig. 2b, c and d). We confirmed that 13 of 19 WNT genes were expressed at low or undetectable levels in SKOV3 and HEY cells (Supplemental Fig. 2). *WNT5A* was detectable in IGROV-1 cells and its mRNA level was approximately 18-fold higher than that in SKOV3.ip1 cells. *WNT5B* was detectable in SKOV3 and HEY cells and its mRNA level was approximately 20-fold higher than that in SKOV3.ip1 cells. However, *WNT5A* and *WNT5B* act through the non-canonical planar cell polarity pathway, not through the canonical WNT/β-catenin pathway. Further, overexpression of WNT7A did not affect *WNT5B* expression in SKOV3 cells. *WNT2B*, *WNT3A*, *WNT7B* and *WNT10A* were 5–15-fold higher in SKOV3.ip1 than in SKOV3 and HEY cells. However, again, loss of WNT7A did not affect any other *WNT* genes in SKOV3.ip1 cells. Therefore, the changes observed in the cell function assays are due solely to regulation by WNT7A in the WNT7A knockdown or overexpressing cells, and not due to other endogenous WNTs.

Because WNT7A stimulates cell growth outside of the ovary (18–20), we first assessed cell proliferation either by counting total cell numbers at 24, 48 and 72 h, or by BrdU incorporation at 48 h (Fig. 2b). Loss of WNT7A in SKOV3.ip1 cells decreased cell numbers after 48 and 72 h compared with control cells ($P<0.05$). Consistent with this result, overexpression of WNT7A in SKOV3 cells increased cell numbers after 24, 48 and 72 h compared to empty vector control transfected cells ($P<0.05$). BrdU incorporation was reduced by loss of WNT7A in SKOV3.ip1 cells, and increased by overexpression of WNT7A in SKOV3 cells at 48 h ($P<0.05$), suggesting that the changes in cell number were the result of altered proliferation rate in cells with both overexpression and loss of WNT7A. To confirm this, cell doubling times were calculated during the exponential growth phase (Fig. 2b). Loss of WNT7A in SKOV3.ip1 cells resulted in significantly longer cell doubling times of 42 h (#11) and 33 h (#12) compared to 23 h for control cells ($P<0.05$). Overexpression of WNT7A in SKOV3 cells resulted in shorter cell doubling times of 34 h (B2) and 25 h (E1) compared with 55 h for pcDNA3.1 vector control cells ($P<0.05$). Next, we examined whether WNT7A can affect the cell cycle distribution of ovarian cancer cells (Supplemental Fig. 3). Loss of WNT7A decreased the proportion of cells in the G_0/G_1 and S phases ($P<0.05$), with a concomitant increase in cells in G_2-phase ($P<0.05$), compared with control cells. In contrast, overexpression of WNT7A increased the proportion of cells in the G_0/G_1 ($P<0.05$), and decreased in the G_2/M transition ($P<0.05$). These changes might be mediated by cyclin D1 which we report to mimic expression level of WNT7A. The importance of cyclin D1 in cell transition through the phases of the cell cycle has been widely recognized (33). Thus, these results suggest that WNT7A stimulates cell proliferation by altering cell cycle distribution through upregulation of cyclin D1.

To assess the potential role of WNT7A in cell dissemination into the peritoneal space and metastasis, we determined whether WNT7A affects cell adhesion and invasion of ovarian carcinoma cells. In solid-phase cell attachment assays (Fig. 2c), we found that overexpression of WNT7A in SKOV3 cells (B2 and E1) increased cell adhesion compared to empty vector control cells ($P<0.05$), whereas knockdown of WNT7A reduced cell attachment in both #11 and #12 clones, as compared to control cells ($P<0.05$). The effects of

WNT7A on cell invasion were measured by a matrigel-coated transwell assay (Fig. 2d). Cell invasion increased approximately 4-fold ($P<0.01$) in WNT7A overexpressing SKOV3 cells (B2 and E1) compared with pcDNA3.1 vector control. In contrast, cell invasion decreased by 60% in WNT7A knockdown SKOV3.ip1 cells (#11 and #12, $P<0.01$). Thus, WNT7A regulates cell adhesion and invasion in ovarian cancer cells, suggesting that WNT7A might not only promote ovarian cancer growth but also potentiate tumor dissemination.

WNT7A regulates tumor growth and progression in vivo

To determine the functional role of WNT7A on ovarian tumor growth, we injected nude mice i.p. with SKOV3.ip1 control or WNT7A knockdown cells (#11 or #12). After 5 weeks, we observed a significant difference in the pattern of tumor growth. Mice injected with control cells developed many large tumors in the omentum, abdominopelvic region, and numerous tumors studding the mesentery adjacent to the bowel (Fig. 3a). Further, unmodified SKOV3.ip1 cells generated several tumor masses invading into the bowel as was determined upon histological examination (Fig. 3b). The average number of tumor implants from injection of control cells was 61.3 ± 10.8, and total tumor weight was 863 ± 75 mg (Fig. 3c). Mice injected with WNT7A knockdown cells typically developed only one large tumor in the retroperitoneal space (data not shown), but significantly fewer implants on the mesentery and abdominopelvic region than control (9.6 ± 3.5 implants, $P<0.01$ vs. control; Fig. 3a and c). The total tumor weight was also 7.2-fold decreased in mice injected with WNT7A knockdown cells (155–168 mg, $P<0.01$ vs. control; Fig. 3c). No tumors invading into the bowel were observed in any of the mice injected with WNT7A knockdown cells (Fig. 3b). While mice injected with control cells did not gain or tended to lose weight due to their illness, mice injected with WNT7A knockdown cells gained 20 ± 1.4 % (clone #11) and 15 ± 1.5 % (clone #12) body weight at 5 weeks after i.p. injection ($P<0.05$; Fig. 3d).

Similar differences in growth of SKOV3.ip1 and WNT7A-suppressed SKOV3.ip1 derivative lines were also observed after s.c. implantation. Tumors derived from WNT7A knockdown cells were significantly smaller starting from day 22 (clone #11) or day 24 (clone #12) compared with control mice ($P<0.05$; Fig. 4a). Tumor weight at 6 weeks after s.c. injection was lower by 62% (clone #11) or 73% (clone #12) in mice injected with WNT7A knockdown cells ($P<0.05$; Fig. 4b). Moreover, significant differences were observed in cyclin D1 expression that was abundantly present in tumors from mice injected with control cells, but relatively low or absent in tumors generated by SKOV3.ip1 with WNT7A knockdown lines (Fig. 4c).

Tumor growth regulated by WNT7A was confirmed by overexpression of WNT7A in SKOV3 cells after s.c. or i.p. implantation (Fig. 5). Tumors derived from WNT7A overexpressing cells were significantly larger starting from day 20 (both B2 and E1), compared to empty vector control tumors ($P<0.05$; Fig. 5a, b and c). Tumor weight at 9 weeks after s.c. injection was higher by 7-fold (clone B2) or 12-fold (clone E1) in mice injected with WNT7A overexpressing cells ($P<0.05$; Fig. 5a and b). Cyclin D1 expression was also increased in tumors generated by SKOV3 with WNT7A overexpressing lines (Fig. 5d). Although tumor growth and progression in the peritoneum was slower than that seen with SKOV3.ip1 cells, we did observe the presence of small tumors growing on the mesentery adjacent to the bowel in mice injected with WNT7A overexpressing cells 10 weeks after i.p. injection (Fig. 5e). The number of implanted tumors in mice injected with WNT7A overexpressing cells (B2, 17.0 ± 4.5; E1, 39.7 ± 16.4 implants) were significantly higher in the mesentery and abdominopelvic region than those in vector control (1.3 ± 0.5 implants, $P<0.05$ vs. control; Fig. 5e).

WNT7A activates the WNT/β-catenin/TCF signaling pathway via FZD5

Next, we assessed whether WNT7A activates the β-catenin-TCF/LEF signaling pathway, using transient transfection with an established TCF/LEF Top-Flash luciferase reporter (Fig. 6a). The TopFlash construct contains T-cell factor binding sites, which are directly activated by the T-cell factor/β-catenin complex (34). The Fop-Flash construct containing mutated T-cell factor–binding sites, served as a negative control. The activity of the TCF/LEF reporter was significantly stimulated by overexpression of WNT7A in SKOV3 (3.7-fold, $P<0.05$) and HEY (4.4-fold, $P<0.05$) cells. Co-transfection with WNT7A and FZD5 further increased stimulation of the TCF/LEF reporter in SKOV3 (6.9-fold, $P<0.05$) and HEY (11.0-fold, $P<0.05$) cells. Transfection of FZD5 alone failed to induce reporter activity. Because SKOV3 and HEY cells do not significantly express endogenous WNTs (Supplemental Fig. 2), it is not likely that the binding of endogenous WNTs to FZD5 accounts for the increase in Top-Flash activity when FZD5 is transfected alone. Further, stimulated Top-Flash reporter activity by WNT7A and FZD5 was inhibited by co-transfection with SFRP2, a WNT receptor antagonist, or dnTCF4 in SKOV3 and HEY cells ($P<0.01$). We also co-transfected with WNT7A and FZD10, because Carmon et al. showed that WNT7A signaling was mediated by FZD5 and FZD10 in endometrial cancer cells (20, 21). However, we did not see any significant Top-Flash activity when cells were co-transfected with FZD10 (data not shown). The β-catenin encoding S33Y construct served as a positive control for the TopFlash reporter. In support of WNT7A regulation of downstream signaling, accumulation of β-catenin in the nucleus faithfully paralleled genetically manipulated WNT7A expression in SKOV3 and SKOV3.ip1 cells following overexpression or knockdown, respectively, however, cytoplasmic β-catenin in cells with altered WNT7A expression was not affected (Fig. 6b).

We also examined β-catenin immunoreactivity in serous carcinomas using anti-active β-catenin (clone 8E7) from Millipore (original from Upstate). The specificity of this antibody is amino acid residues 36–44 (HSGATTTAP) of human β-catenin, Mr 92kDa, specific for the active form of β-catenin dephosphorylated on Ser37 or Thr41. This antibody was used to determine the nuclear localization of β-catenin (35). We were able to detect nuclear β-catenin in serous carcinomas (Supplemental Fig. 4). Nuclear localization of CTNNB1 was observed in 25/36 total serous specimens investigated. The ratio of nuclear CTNNB1 positive tumors (69%) was similar to that of WNT7A positive tumors (65%). Although the tumor panel screen for *WNT7A* expression by *in situ* hybridization and immunohistochemistry to detect nuclear β-catenin were performed independently, 7 distinct cases of serous carcinomas were in common between the two arrays. Interestingly, 5 of 7 were strongly positive for both *WNT7A* and nuclear β-catenin (Supplemental Fig. 4).

Because it has been noted in endometrioid ovarian carcinoma that CTNNB1 can be activated via constitutive mutations rather than activation of its normal signaling pathway (10). We examined the mutation status in 25 serous carcinoma samples in which we detected nuclear localization of CTNNB1. We did not see evidence of mutations in the 3 “activation” hot spots (codons 33, 34 and 37 of Exon 3), nor in the flanking sequence, in eighteen samples (suitable sequence was unable to be obtained from 7/25 samples). The 18 samples analyzed included the 5 samples that were strongly positive for both *WNT7A* and nuclear β-catenin, and no mutations were observed. In addition, we determined that the activation of the β-catenin pathway in our *in vitro* experiments was also not due to mutations, as none of the cells lines (SKOV3, SKOV3.ip1, IGROV-1, and HEY) harbored sequence changes in exon 3 (data not shown). In contrast, TOV-112D cells were confirmed to have activating mutation in exon 3 that stimulated Top-Flash reporter activity (data not shown) as previously reported (31). Taken in total, these results provide three lines of evidence that serous ovarian cancer tumors have an intact β-catenin-TCF/LEF signaling pathway which can potentially be activated by WNT7A.

WNT7A stimulates MMP7 promoter

To determine a downstream target of WNT7A signaling that can translate the effects of the β-catenin pathway, we examined MMP7, which is an established WNT/β-catenin target gene (7, 36) and one of the few MMP family members expressed in the epithelium (37, 38). Robust MMP7 expression correlated with WNT7A expression levels in SKOV3.ip1 cells (Supplemental Fig. 1b). MMP7 is a soluble metalloproteinase that has been repeatedly linked to tumor progression and metastasis in various types of cancers (39). We, therefore, hypothesized that WNT7A-induced upregulation of MMP7 might confer a more aggressive growth phenotype in ovarian tumors *in vivo*. To test this hypothesis, we first examined whether WNT7A activates the MMP7 promoter in ovarian cancer cells. HEY cells were used for this study due to their low or undetectable levels of endogenous WNT7A and higher levels of endogenous MMP7 than those found in SKOV3 cells. Promoter activity was determined by comparing the relative luciferase activity from constructs containing different lengths of MMP7 5′-flanking sequences in transiently transfected HEY cells in the presence of WNT7A or control expression vectors (Fig. 7). Both the -535 and -204 nt promoter constructs expressed 2.3 and 2.5-fold, respectively, higher luciferase activity when WNT7A was overexpressed ($P<0.05$). This activation was specifically mediated by TCF binding sites because a shortened promoter lacking -204 to -62 segments with putative TCF sites (36) reduced the promoter's activity level to baseline (Fig. 7a and b). Furthermore, mutation of either of these TCF binding sites reduced luciferase activity by 69–76% ($P<0.05$) despite WNT7A overexpression (Fig. 7c). Thus, these results provide the first molecular evidence that activation of β-catenin-TCF/LEF signaling by WNT7A stimulates MMP7 promoter and increases MMP7 expression in ovarian cancer cells.

Discussion

While the progression of cancer in general has been frequently attributed to constitutive activation of β-catenin via WNT pathways (12, 31, 40), the specific ligand partners associated with WNT signaling in ovarian cancer have not been identified. We postulate that WNT7A is one of the WNT ligands that can contribute to generation and formation of ovarian cancer in human patients. This conclusion is based on several pieces of evidence presented here. First, we found that WNT7A is abundantly expressed in ovarian malignant tumors, but absent in normal ovary. Second, we also found that WNT7A has the capacity to control cell division by altering cell cycle distribution, cell adhesion, and directional cell motility. Third, we showed in orthotopic ovarian xenograft models *in vivo* that WNT7A knockdown cancer cells have significantly decreased rate of growth, invasion and dissemination throughout the peritoneal cavity, and WNT7A overexpressing cells exhibit increased tumor growth. Fourth, we demonstrate here on a transcriptional level that WNT7A activates the canonical WNT/β-catenin signaling pathway in ovarian cancer cells, and stimulates target genes that are critical for tumor growth and metastasis. Taken together, these findings suggest that WNT7A has an important role in the growth and progression of human ovarian malignancies.

Screening for the spatial expression of *WNT7A* in human specimens of ovarian cancer revealed that approximately 65% of serous adenocarcinomas expressed *WNT7A* with particularly strong expression. WNT7A upregulation has been reported in endometrial cancer (21) where its expression is exclusively restricted to epithelial cells (13–16, 21). Interestingly, WNT7A expression was not detected in the majority of endometrioid carcinomas, although mutations in β-catenin are known to be present in more than 60% of ovarian endometrioid carcinomas and their precursor lesions (10, 41, 42). It has been previously suggested that the formation of endometrioid carcinomas is promoted by β-catenin mutations and constitutive activation of its downstream signaling (11, 43, 44). However, nuclear localization of β-catenin has been reported in not only endometrioid, but

also serous carcinomas (12). We show here that nuclear accumulation of β-catenin in ovarian cancer cells is regulated by WNT7A. Thus, our studies support a novel mechanism promoting growth of serous carcinomas that might result from overstimulation of the intact β-catenin pathway following overexpression of WNT7A.

The results from analysis of clinical specimens were consistent with the data derived from the xenograft models, further supporting the idea of WNT7A is a potential tumor promoting factor in EOC. Subcutaneously implanted SKOV3.ip1 tumors with suppressed WNT7A had a significantly slower growth rate concomitant with reduced expression of cyclin D1. These results were confirmed by overexpression of WNT7A as well. This finding suggests that WNT7A can promote cancer cell proliferation through alteration of cell cycle G_1/S transition via accumulation of cyclin D1. It is well known that the relative expression pattern of cyclin D1 is critical for cell cycle progression (45). Cyclin D1 expression is high during the G_0/G_1 phase, allowing cells to enter S phase and replicate DNA, whereas its levels drop very low before rising again during G_2 (45). In the present study, cyclin D1 levels paralleled those of WNT7A in overexpressed and knocked down cancer cells, and high expression of both proteins correlated with accumulation of cell populations in both the G_0/G_1 and S phases. Thus, these results suggest that the control of cyclin D1 expression by WNT7A accelerates cell cycle in ovarian cancer cells, leading to increase proliferation noticed in both *in vitro* and *in vivo* settings.

In addition to increased proliferation, we found that WNT7A expression also affected the growth pattern of peritoneal lesions generated by SKOV3.ip1 tumors. As compared with unmodified SKOV3.ip1 cells, mice injected with WNT7A knockdown cells showed only few or no tumors in the peritoneal cavity. This observation suggested that WNT7A might regulate cancer cell adhesion and invasion, two critical processes for ovarian tumor dissemination and metastasis that require tumor cells to attach and invade to the peritoneum and omentum. The results from *in vitro* experiments showed, indeed, that WNT7A has a significant capacity to regulate both adhesion and invasion of ovarian cancer lines. Thus, WNT7A's potential role in governing cell adhesion and invasion may be preserved *in vivo* where disseminated tumor cells in the peritoneal cavity attach to the peritoneum and omentum, and invade into the secondary organs.

We examined several downstream targets of WNT signaling that can translate the effects of the β-catenin pathway into enhanced tumor growth and metastatic pattern observed *in vivo*. One of the targets that attracted our attention was a metalloproteinase gene, MMP7, also known as matrilysin. MMP7 has been linked to activation of the β-catenin pathway, and is well known to be associated with invasion and metastasis in a variety of cancers including those of stomach (46), colon (47, 48) and pancreas (49). MMP7 is one of the few MMP family members expressed in the epithelium, and promotes migration and invasion of tumor cells via extracellular cleavage of E-cadherin (37, 38). MMP7 is also known to activate other MMPs, such as proMMP2 and proMMP9, which additionally facilitate tumor invasion (50). We found that MMP7 was robustly expressed in parental SKOV3.ip1 cells, and its expression level was correspondingly changed by overexpression or knockdown of WNT7A. Further, overexpression of WNT7A in ovarian cancer cells stimulated the MMP7 promoter, and mutation of TCF binding sites in the MMP7 promoter confirmed that activation of MMP7 promoter by WNT7A was mediated by β-catenin-TCF signaling. Thus, these results suggest that MMP7 is a downstream target of WNT7A signaling in ovarian cancer, and its function can promote tumor invasion and dissemination into secondary sites.

The important conclusion of this study is that abundant WNT7A is present in human specimens of EOC. We also show that WNT7A in ovarian cancer cells activates the WNT/β-catenin signaling pathway and directly promotes cell functions associated with tumor growth

in vivo. Further, WNT7A regulates the pattern of diffuse tumor growth and dissemination. These effects can be mediated by upregulation of cyclin D1 and MMP7, leading to both cell cycle and migratory/invading program in ovarian cancer cells. Thus, the present results lay the foundation for future studies on the mechanisms of WNT7A induced activation of the WNT/β-catenin pathway in formation and progression of ovarian cancer in human patients. Further, the present study also suggests that WNT7A is an important novel target for developing therapeutic strategies to suppress ovarian cancer growth and spread.

Supplementary Material

Refer to Web version on PubMed Central for supplementary material.

Acknowledgments

This work was supported in part by American Cancer Society Illinois Division #139038, NIH/NICHD HD058222, and SIU-SOM Central Research Committee (to KH).

References

1. Jemal A, Siegel R, Xu J, Ward E. Cancer Statistics, 2010. CA Cancer J Clin. 2010 Jul 7.
2. Bell DA. Origins and molecular pathology of ovarian cancer. Mod Pathol. 2005 Feb; 18(Suppl 2):S19–32. [PubMed: 15761464]
3. Lee HY, Kleber M, Hari L, Brault V, Suter U, Taketo MM, et al. Instructive role of Wnt/beta-catenin in sensory fate specification in neural crest stem cells. Science. 2004 Feb 13; 303(5660): 1020–3. [PubMed: 14716020]
4. Teo R, Mohrlen F, Plickert G, Muller WA, Frank U. An evolutionary conserved role of Wnt signaling in stem cell fate decision. Dev Biol. 2006 Jan 1; 289(1):91–9. [PubMed: 16309665]
5. Polakis P. Wnt signaling and cancer. Genes Dev. 2000 Aug 1; 14(15):1837–51. [PubMed: 10921899]
6. Nusse R, Varmus HE. Many tumors induced by the mouse mammary tumor virus contain a provirus integrated in the same region of the host genome. Cell. 1982 Nov; 31(1):99–109. [PubMed: 6297757]
7. Crawford HC, Fingleton BM, Rudolph-Owen LA, Goss KJ, Rubinfeld B, Polakis P, et al. The metalloproteinase matrilysin is a target of beta-catenin transactivation in intestinal tumors. Oncogene. 1999 May 6; 18(18):2883–91. [PubMed: 10362259]
8. He TC, Sparks AB, Rago C, Hermeking H, Zawel L, da Costa LT, et al. Identification of c-MYC as a target of the APC pathway. Science. 1998 Sep 4; 281(5382):1509–12. [PubMed: 9727977]
9. Shtutman M, Zhurinsky J, Simcha I, Albanese C, D'Amico M, Pestell R, et al. The cyclin D1 gene is a target of the beta-catenin/LEF-1 pathway. Proceedings of the National Academy of Sciences of the United States of America. 1999 May 11; 96(10):5522–7. [PubMed: 10318916]
10. Cho KR. Ovarian cancer update: lessons from morphology, molecules, and mice. Arch Pathol Lab Med. 2009 Nov; 133(11):1775–81. [PubMed: 19886711]
11. Kildal W, Risberg B, Abeler VM, Kristensen GB, Sudbo J, Nesland JM, et al. beta-catenin expression, DNA ploidy and clinicopathological features in ovarian cancer: a study in 253 patients. Eur J Cancer. 2005 May; 41(8):1127–34. [PubMed: 15911235]
12. Lee CM, Shvartsman H, Deavers MT, Wang SC, Xia W, Schmandt R, et al. beta-catenin nuclear localization is associated with grade in ovarian serous carcinoma. Gynecol Oncol. 2003 Mar; 88(3):363–8. [PubMed: 12648588]
13. Hayashi K, Spencer TE. WNT pathways in the neonatal ovine uterus: potential specification of endometrial gland morphogenesis by SFRP2. Biology of reproduction. 2006 Apr; 74(4):721–33. [PubMed: 16407498]
14. Miller C, Sassoon DA. Wnt-7a maintains appropriate uterine patterning during the development of the mouse female reproductive tract. Development. 1998; 125(16):3201–11. [PubMed: 9671592]

15. Tulac S, Nayak NR, Kao LC, Van Waes M, Huang J, Lobo S, et al. Identification, characterization, and regulation of the canonical Wnt signaling pathway in human endometrium. J Clin Endocrinol Metab. 2003 Aug; 88(8):3860–6. [PubMed: 12915680]
16. Hayashi K, Erikson DW, Tilford SA, Bany BM, Maclean JA 2nd, Rucker EB 3rd, et al. Wnt genes in the mouse uterus: potential regulation of implantation. Biology of reproduction. 2009 May; 80(5):989–1000. [PubMed: 19164167]
17. Hayashi K, Yoshioka S, Reardon SN, Rucker EB 3rd, Spencer TE, Demayo FJ, et al. WNTs in the Neonatal Mouse Uterus: Potential Regulation of Endometrial Gland Development. Biology of reproduction. 2011 Oct 20.
18. Hayashi K, Burghardt RC, Bazer FW, Spencer TE. WNTs in the ovine uterus: potential regulation of periimplantation ovine conceptus development. Endocrinology. 2007 Jul; 148(7):3496–506. [PubMed: 17431004]
19. Lyu J, Joo CK. Wnt-7a up-regulates matrix metalloproteinase-12 expression and promotes cell proliferation in corneal epithelial cells during wound healing. J Biol Chem. 2005 Jun 3; 280(22): 21653–60. [PubMed: 15802269]
20. Carmon KS, Loose DS. Wnt7a interaction with Fzd5 and detection of signaling activation using a split eGFP. Biochem Biophys Res Commun. 2008 Apr 4; 368(2):285–91. [PubMed: 18230341]
21. Carmon KS, Loose DS. Secreted frizzled-related protein 4 regulates two wnt7a signaling pathways and inhibits proliferation in endometrial cancer cells. Mol Cancer Res. 2008 Jun; 6(6):1017–28. [PubMed: 18567805]
22. Yu D, Wolf JK, Scanlon M, Price JE, Hung MC. Enhanced c-erbB-2/neu expression in human ovarian cancer cells correlates with more severe malignancy that can be suppressed by E1A. Cancer research. 1993 Feb 15; 53(4):891–8. [PubMed: 8094034]
23. Benard J, Da Silva J, De Blois MC, Boyer P, Duvillard P, Chiric E, et al. Characterization of a human ovarian adenocarcinoma line, IGROV1, in tissue culture and in nude mice. Cancer research. 1985 Oct; 45(10):4970–9. [PubMed: 3861241]
24. Spencer TE, Stagg AG, Joyce MM, Jenster G, Wood CG, Bazer FW, et al. Discovery and characterization of endometrial epithelial messenger ribonucleic acids using the ovine uterine gland knockout model. Endocrinology. 1999 Sep; 140(9):4070–80. [PubMed: 10465278]
25. Chauhan SC, Vannatta K, Ebeling MC, Vinayek N, Watanabe A, Pandey KK, et al. Expression and functions of transmembrane mucin MUC13 in ovarian cancer. Cancer research. 2009 Feb 1; 69(3): 765–74. [PubMed: 19176398]
26. Singh AP, Moniaux N, Chauhan SC, Meza JL, Batra SK. Inhibition of MUC4 expression suppresses pancreatic tumor cell growth and metastasis. Cancer research. 2004 Jan 15; 64(2):622–30. [PubMed: 14744777]
27. Bayless KJ, Meininger GA, Scholtz JM, Davis GE. Osteopontin is a ligand for the alpha4beta1 integrin. J Cell Sci. 1998 May; 111(Pt 9):1165–74. [PubMed: 9547293]
28. Langlois MJ, Bergeron S, Bernatchez G, Boudreau F, Saucier C, Perreault N, et al. The PTEN phosphatase controls intestinal epithelial cell polarity and barrier function: role in colorectal cancer progression. PLoS One. 2010; 5(12):e15742. [PubMed: 21203412]
29. Wang FQ, Fisher J, Fishman DA. MMP-1-PAR1 axis mediates LPA-induced epithelial ovarian cancer (EOC) invasion. Gynecol Oncol. 2011 Feb; 120(2):247–55. [PubMed: 21093894]
30. Satpathy M, Cao L, Pincheira R, Emerson R, Bigsby R, Nakshatri H, et al. Enhanced peritoneal ovarian tumor dissemination by tissue transglutaminase. Cancer research. 2007 Aug 1; 67(15): 7194–202. [PubMed: 17671187]
31. Wu R, Zhai Y, Fearon ER, Cho KR. Diverse mechanisms of beta-catenin deregulation in ovarian endometrioid adenocarcinomas. Cancer research. 2001 Nov 15; 61(22):8247–55. [PubMed: 11719457]
32. Bui TD, Zhang L, Rees MC, Bicknell R, Harris AL. Expression and hormone regulation of Wnt2, 3, 4, 5a, 7a, 7b and 10b in normal human endometrium and endometrial carcinoma. Br J Cancer. 1997; 75(8):1131–6. [PubMed: 9099960]
33. Stacey DW. Cyclin D1 serves as a cell cycle regulatory switch in actively proliferating cells. Curr Opin Cell Biol. 2003 Apr; 15(2):158–63. [PubMed: 12648671]

34. Veeman MT, Slusarski DC, Kaykas A, Louie SH, Moon RT. Zebrafish prickle, a modulator of noncanonical Wnt/Fz signaling, regulates gastrulation movements. Curr Biol. 2003 Apr 15; 13(8): 680–5. [PubMed: 12699626]
35. Hou X, Tan Y, Li M, Dey SK, Das SK. Canonical Wnt signaling is critical to estrogen-mediated uterine growth. Mol Endocrinol. 2004 Dec; 18(12):3035–49. [PubMed: 15358837]
36. Brabletz T, Jung A, Dag S, Hlubek F, Kirchner T. beta-catenin regulates the expression of the matrix metalloproteinase-7 in human colorectal cancer. Am J Pathol. 1999 Oct; 155(4):1033–8. [PubMed: 10514384]
37. Davies G, Jiang WG, Mason MD. Matrilysin mediates extracellular cleavage of E-cadherin from prostate cancer cells: a key mechanism in hepatocyte growth factor/scatter factor-induced cell-cell dissociation and in vitro invasion. Clin Cancer Res. 2001 Oct; 7(10):3289–97. [PubMed: 11595727]
38. Noe V, Fingleton B, Jacobs K, Crawford HC, Vermeulen S, Steelant W, et al. Release of an invasion promoter E-cadherin fragment by matrilysin and stromelysin-1. J Cell Sci. 2001 Jan; 114(Pt 1):111–8. [PubMed: 11112695]
39. Ii M, Yamamoto H, Adachi Y, Maruyama Y, Shinomura Y. Role of matrix metalloproteinase-7 (matrilysin) in human cancer invasion, apoptosis, growth, and angiogenesis. Exp Biol Med (Maywood). 2006 Jan; 231(1):20–7. [PubMed: 16380641]
40. Sarrio D, Moreno-Bueno G, Sanchez-Estevez C, Banon-Rodriguez I, Hernandez-Cortes G, Hardisson D, et al. Expression of cadherins and catenins correlates with distinct histologic types of ovarian carcinomas. Hum Pathol. 2006 Aug; 37(8):1042–9. [PubMed: 16867867]
41. Kim H, Wu R, Cho KR, Thomas DG, Gossner G, Liu JR, et al. Comparative proteomic analysis of low stage and high stage endometrioid ovarian adenocarcinomas. Proteomics Clin Appl. 2008 Mar 7; 2(4):571–84. [PubMed: 20523764]
42. Shih Ie M, Kurman RJ. Ovarian tumorigenesis: a proposed model based on morphological and molecular genetic analysis. Am J Pathol. 2004 May; 164(5):1511–8. [PubMed: 15111296]
43. Gatcliffe TA, Monk BJ, Planutis K, Holcombe RF. Wnt signaling in ovarian tumorigenesis. Int J Gynecol Cancer. 2008 Sep–Oct; 18(5):954–62. [PubMed: 17986238]
44. Schwartz DR, Wu R, Kardia SL, Levin AM, Huang CC, Shedden KA, et al. Novel candidate targets of beta-catenin/T-cell factor signaling identified by gene expression profiling of ovarian endometrioid adenocarcinomas. Cancer research. 2003 Jun 1; 63(11):2913–22. [PubMed: 12782598]
45. Yang K, Hitomi M, Stacey DW. Variations in cyclin D1 levels through the cell cycle determine the proliferative fate of a cell. Cell Div. 2006; 1:32. [PubMed: 17176475]
46. Aihara R, Mochiki E, Nakabayashi T, Akazawa K, Asao T, Kuwano H. Clinical significance of mucin phenotype, beta-catenin and matrix metalloproteinase 7 in early undifferentiated gastric carcinoma. Br J Surg. 2005 Apr; 92(4):454–62. [PubMed: 15609380]
47. Adachi Y, Yamamoto H, Itoh F, Arimura Y, Nishi M, Endo T, et al. Clinicopathologic and prognostic significance of matrilysin expression at the invasive front in human colorectal cancers. Int J Cancer. 2001 Sep 20; 95(5):290–4. [PubMed: 11494227]
48. Yamamoto H, Itoh F, Adachi Y, Sakamoto H, Adachi M, Hinoda Y, et al. Relation of enhanced secretion of active matrix metalloproteinases with tumor spread in human hepatocellular carcinoma. Gastroenterology. 1997 Apr; 112(4):1290–6. [PubMed: 9098015]
49. Jones LE, Humphreys MJ, Campbell F, Neoptolemos JP, Boyd MT. Comprehensive analysis of matrix metalloproteinase and tissue inhibitor expression in pancreatic cancer: increased expression of matrix metalloproteinase-7 predicts poor survival. Clin Cancer Res. 2004 Apr 15; 10(8):2832–45. [PubMed: 15102692]
50. Wang FQ, So J, Reierstad S, Fishman DA. Matrilysin (MMP-7) promotes invasion of ovarian cancer cells by activation of progelatinase. Int J Cancer. 2005 Mar 10; 114(1):19–31. [PubMed: 15523695]

a

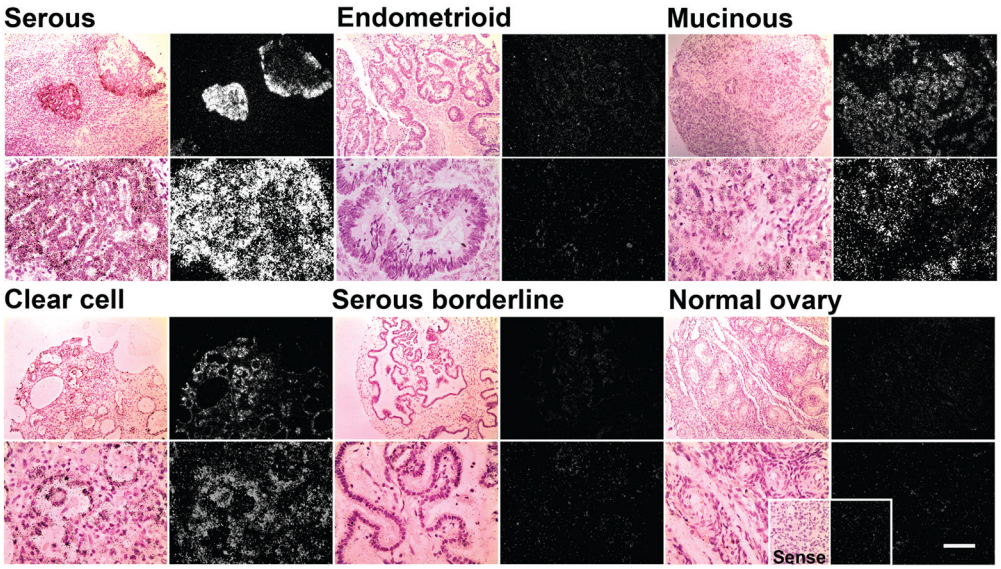

b

	Serous	Endometrioid	Mucinous	Clear cell	Serous benign/borderline	Endometrioid benign/borderline	Normal ovary
+++	29 (15.3%)	0	1 (5.3%)	1 (4.8%)	0	0	0
++	35 (18.5%)	0	2 (10.5%)	2 (9.5%)	0	0	0
+	37 (19.6%)	2 (3.8%)	1 (5.3%)	2 (9.5%)	0	0	0
+/-	21 (11.1%)	3 (5.8%)	3 (15.8%)	1 (4.8%)	0	0	0
-	67 (35.4%)	47 (90.4%)	12 (63.2%)	15 (71.4%)	3 (100%)	4 (100%)	12 (100%)
total	189	52	19	21	3	4	12

FIGURE 1.

Expression of *WNT7A* in ovarian tumors, borderline and normal ovaries. (a) For each tissue type, representative photomicrographs of *WNT7A* expression are presented in dark-field illumination (right panels), and bright-field photomicrographs (left panels) for comparison of the histology for each section. Scale bar = 100μm. (b) Summary of *WNT7A* expression in ovarian tumors. Distribution and relative abundance of *WNT7A* by phenotype (serous, endometrioid, mucinous and clear cell), borderline and normal ovaries. Relative hybridization signal intensity for mRNA expression of *WNT7A* was assessed visually in each specimen by two independent observers and scored as follows: absent (−), detectable (+/−), weak (+), moderate (++), or strong (+++).

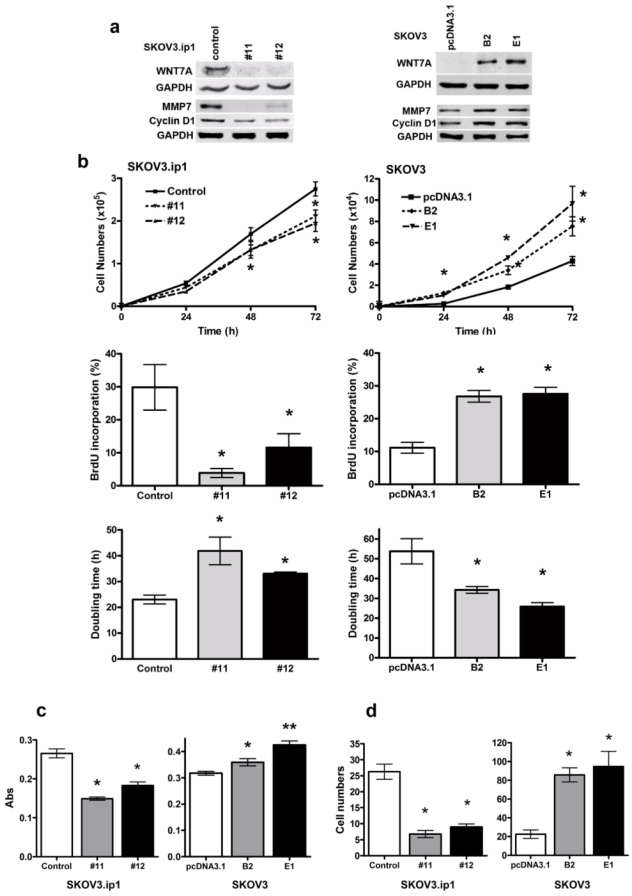

FIGURE 2.

WNT7A-regulated cell proliferation, cell adhesion and invasion in ovarian cancer cells. (a) Protein levels of WNT7A, cyclin D1 and MMP7 in SKOV3.ip1 and SKOV3 cells. To stably knockdown WNT7A, SKOV3.ip1 cells were infected with either control shRNA or 5 different WNT7A shRNAs #11 and #12 or (#8, #9, #10, not shown) by lentiviral particles (MISSION shRNA system, Sigma-Aldrich), and selected by puromycin (500 ng/ml). Puromycin-resistant colonies were selected, expanded individually, and analyzed for WNT7A expression. To stably overexpress WNT7A, SKOV3 cells were transfected using Turbofect, with either empty pcDNA3.1 control vector or WNT7A cloned into pcDNA3.1 vector. Stably transfected clones were selected with G418 (600 μg/ml), expanded individually, and analyzed for WNT7A expression (clones B2 and E1 exhibited highest expression). (b) Cell proliferation was determined by counting total cell numbers at 24, 48 and 72 h of culture. BrdU incorporation during DNA synthesis was measured at 48 h of culture. Doubling time was calculated from the cell growth curve during the exponential growth phase (0–72 h). Values indicate the mean ± SEM, * indicates $P<0.05$ vs. control or pcDNA3.1. (c) Cell adhesion assay was performed in 96-well plates, and attached cells were quantified by Amido Black staining. Values indicate mean ± SEM absorbance readings, * or ** indicates $P<0.05$ or $P<0.001$ vs. control or pcDNA3.1. (d) An invasion assay was done by modified Boyden Chamber coated with matrigel. Cell counts are shown as mean ± SEM * indicates $P<0.01$ vs. control or pcDNA3.1.

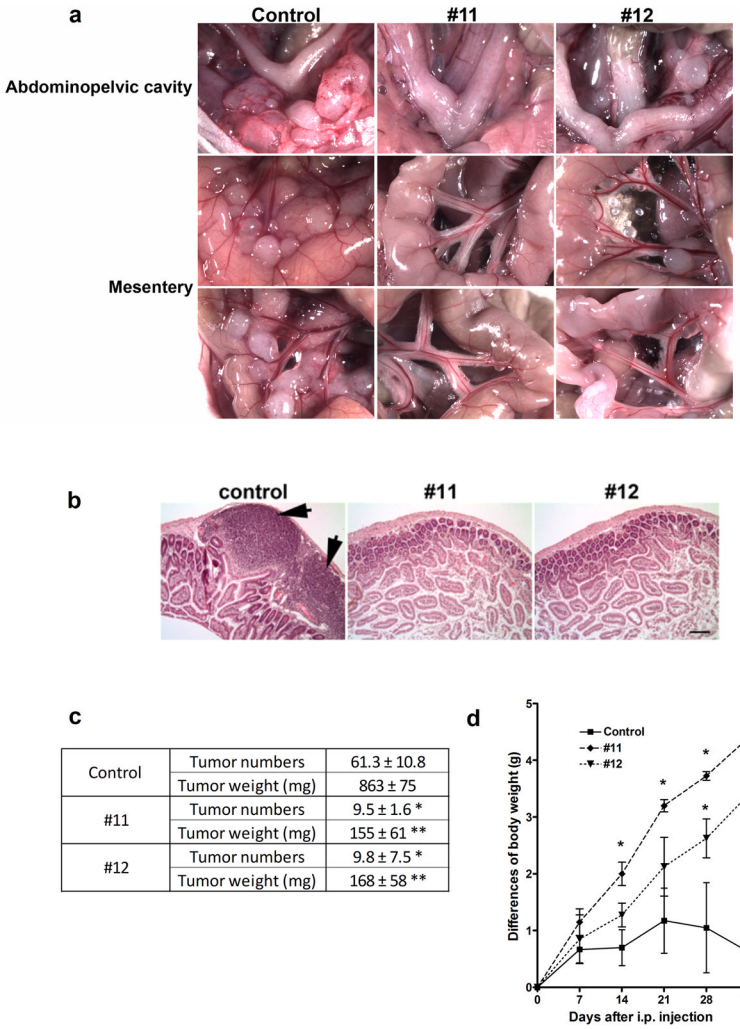

Control	Tumor numbers	61.3 ± 10.8
	Tumor weight (mg)	863 ± 75
#11	Tumor numbers	9.5 ± 1.6 *
	Tumor weight (mg)	155 ± 61 **
#12	Tumor numbers	9.8 ± 7.5 *
	Tumor weight (mg)	168 ± 58 **

FIGURE 3.

WNT7A knockdown inhibits tumor progression. (a) *In vivo* xenograft tumor progression. Nude mice were injected i.p. with control cells or WNT7A knockdown cells (#11 or #12). The images provide a direct view of the area in abdominopelvic cavity around the reproductive tract, and intestinal mesentery. (b) Histological examination of intestine following i.p. injection with control and WNT7A knockdown cells. Scale bar = 100μm. (c) Numbers of implanted tumors and total tumor weight 5 weeks after i.p. injection are shown. Data are presented as average number of implants and weight ± SEM. Individual tumors > 2 mm were included. * or ** vs control, P<0.01. (d) Differences in body weight are shown during 5 weeks. * vs control, P<0.05.

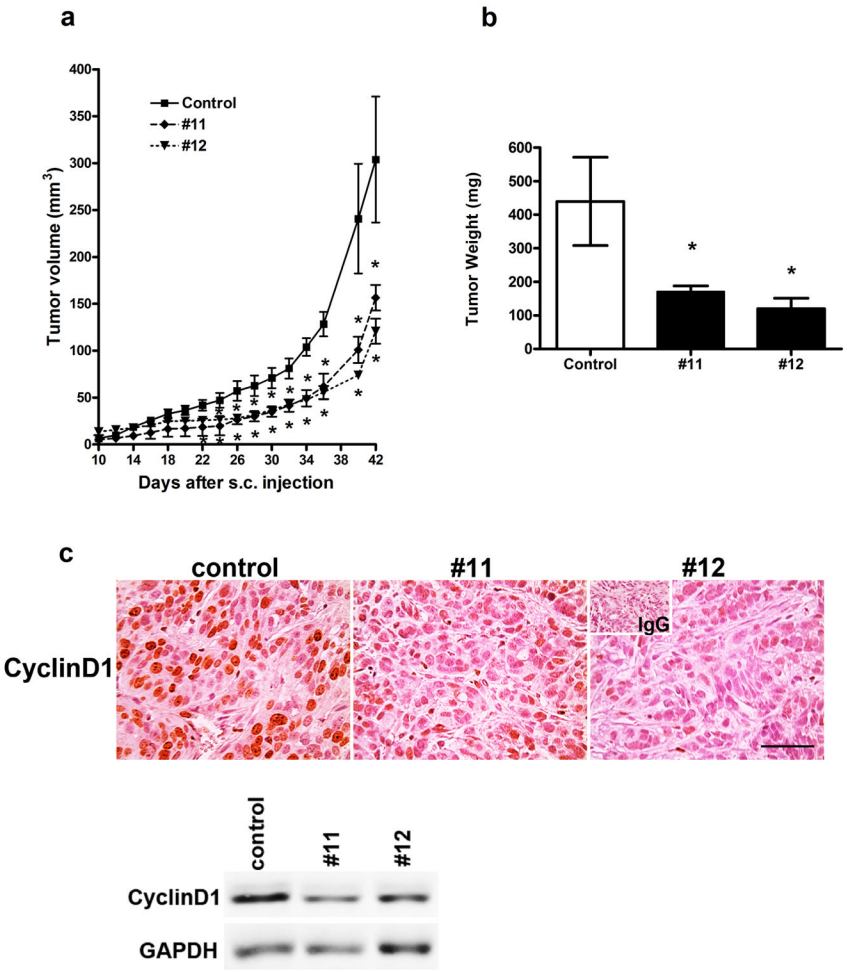

FIGURE 4.

WNT7A knockdown inhibits tumor growth. (a) *In vivo* xenograft tumor growth. Nude mice were injected s.c. with control or WNT7A knockdown cells (#11 or #12). * vs control, $P<0.05$. (b) Final tumor weight 6 weeks after s.c. injection. * vs control, $P<0.05$. (c) Cyclin D1 in s.c. tumors that developed from control and WNT7A knockdown cells was determined by immunohistochemistry and western blot analyses. Scale bar represents 100μm.

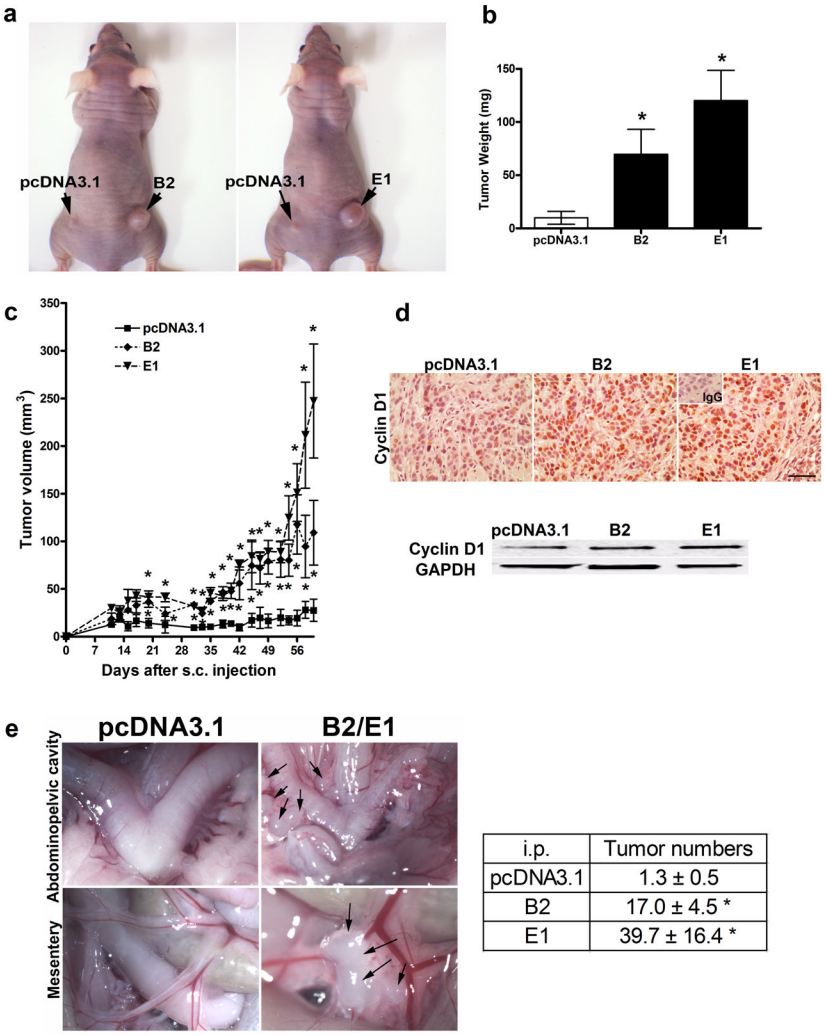

i.p.	Tumor numbers
pcDNA3.1	1.3 ± 0.5
B2	17.0 ± 4.5 *
E1	39.7 ± 16.4 *

FIGURE 5.

WNT7A overexpression increases tumor growth. (ab) *In vivo* xenograft tumor growth. Nude mice were injected s.c. with vector control or WNT7A overexpressing cells (B2 or E1). Final tumor pictures (a) and tumor weight (b) 9 weeks after s.c. injection are shown. * vs pcDNA3.1 vector control, P<0.05. (c) Tumor volume was measured every 2 days 10 days after s.c. injection. * vs pcDNA3.1 vector control, P<0.05. (d) Cyclin D1 expression in s.c. tumors that developed from pcDNA3.1 vector control and WNT7A overexpressed cells was determined by immunohistochemistry and western blot analyses. Scale bar represents 100μm. (e) *In vivo* xenograft tumor progression. Nude mice were injected i.p. with vector control cells or WNT7A overexpressing cells (B2 or E1). The images provide a direct view of the area in abdominopelvic cavity around the reproductive tract, and intestinal mesentery. Numbers of implanted tumors 10 weeks after i.p. injection are shown. Data are presented as average number of implants ± SEM. Individual tumors > 2 mm were calculated. * vs vector control, P<0.05.

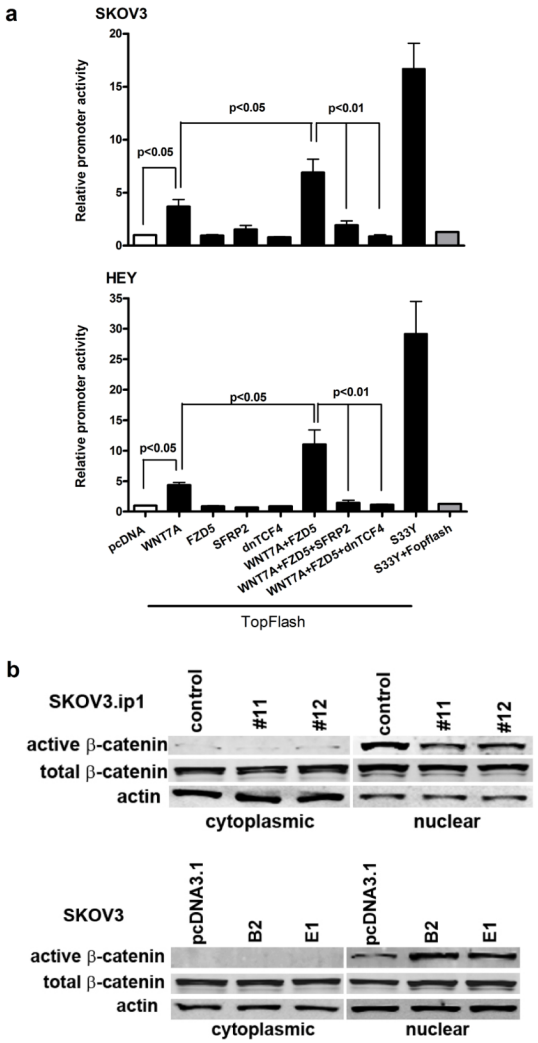

FIGURE 6.

WNT7A activates the β-catenin-TCF/LEF signaling pathway in ovarian cancer cells. (a) To measure WNT/β-catenin signaling in SKOV3 and HEY cells lacking endogenous WNT7A, cells were co-transfected with either empty pcDNA3.1 or one or more of the indicated WNT7A, FZD5, SFRP2, dnTCF4 or S33Y expression vectors in concert with the firefly luciferase-tagged Top-Flash reporter or Fop-Flash as a negative control. Luciferase activity was measured using a Dual-Luciferase Reporter Assay System 24 h after transfection. The results are presented as the mean relative light units per sec (RLU/sec) derived from three independent experiments. Data were arbitrarily set to background level of 1 from luciferase activity transfected with pcDNA3.1 vector. (b) Nuclear or cytoplasmic β-catenin in SKOV3.ip1 control or WNT7A knockdown cells, or SKOV3 control or WNT7A overexpressing cells as determined by western blot analysis.

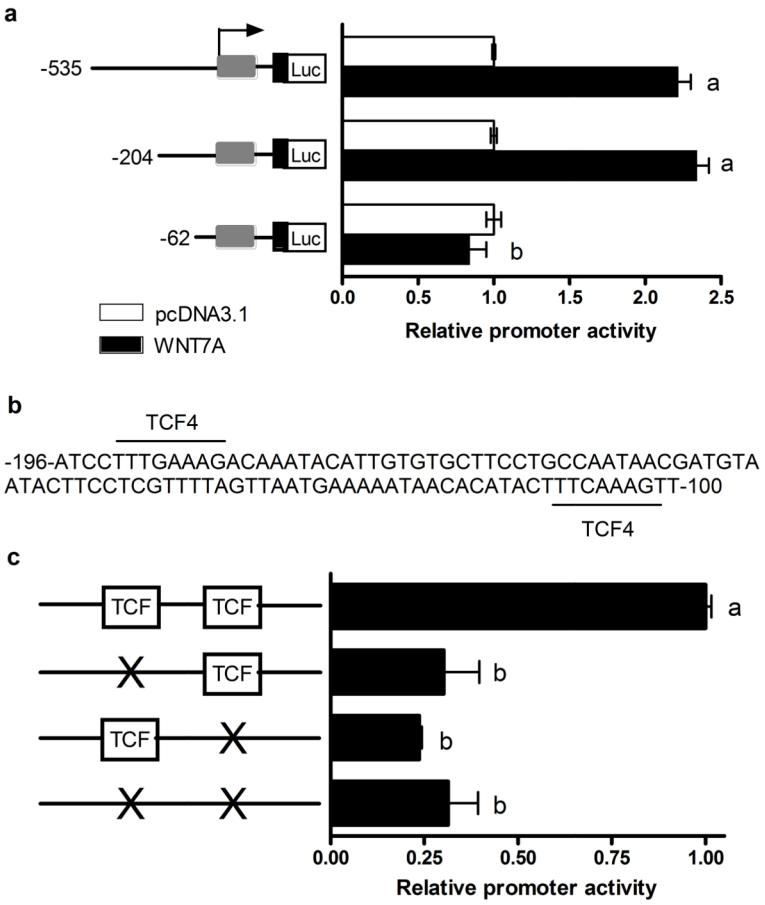

FIGURE 7.

WNT7A stimulates MMP7 promoter that contains TCF binding sites. (a) Promoter activity was determined by comparing the relative luciferase activity from constructs containing -535, -204 and -62 nt of 5′ flanking sequence from the human *MMP7* gene cloned into pGL3-basic transiently transfected with or without co-transfection with WNT7A or control vector in HEY cells. Luciferase activity was measured using a Dual-Luciferase Reporter Assay System 24h after transfection. Results are presented as the mean relative light units per sec (RLU/sec) assayed in duplicate derived from three independent experiments. Data were set to background level of 1 from luciferase activity transfected with pcDNA3.1 vector. a, b; $P<0.05$. (b) The -196 to -100-nt region contains two consensus TCF binding sites. (c) Site-directed mutagenesis of the TCF binding sites abrogates MMP7 promoter activity.